MADRID
inter.noise 2019
June 16 - 19
NOISE CONTROL FOR A BETTER ENVIRONMENT

A Comprehensive Model for the Turbulent Boundary Layer Pressure Spectrum

DeJong, Richard[1]
Tubergen, Renard
Calvin Engineering Department
1712 Knollcrest Circle
Grand Rapids, MI 49546

ABSTRACT

Using test data from wind tunnel and water channel fluid flow tests, the model originally developed by Chase for the low wavenumber spectrum of the pressure in a turbulent boundary layer has been extended to cover the entire wavenumber and frequency range. Particular attention is given to the low wavenumber and high frequency regions. The low wavenumber spectrum level is found to be nearly constant and a theoretical basis for this is proposed. The high frequency spectrum level is found to correlate best with the inner variables (shear stress and viscosity) while the remaining regions correlate best with the outer variables (convection velocity and boundary layer thickness).

Keywords: Flow Noise, Turbulent Boundary Layer
I-INCE Classification of Subject Number: 13, 21

1. INTRODUCTION

The pressure fluctuations in a turbulent boundary layer (TBL) flow over a surface are important sources of structural vibration and transmitted sound. The strength of the excitation depends on both the spatial and temporal matching of the pressure and vibration fields. Typically this is described by functions of wavenumber, k, and frequency, ω, which are Fourier transforms of the spatial and temporal fields, respectively. A typical example of an empirical formula for the pressure spectrum, Φ_p, describing the pressure field in a fully developed TBL is given by the basic Chase model [1]

$$\Phi_p(k,\omega) = C\,\rho_o^2\,u_c^3\,k^2\,[k^2 + (2\pi)^2\,(\omega/u_c - k_x)^2 + \delta^{-2}]^{-5/2} \qquad (1)$$

where ρ_o is the ambient fluid density, u_c is the convection velocity of the turbulence, δ is the effective thickness of the turbulent boundary layer, and C is a constant,.

Of particular interest in the development of Equation 1 was the low wavenumber component of Φ_p which plays an important role in the structural response to TBL pressures in some cases. This is illustrated in Figure 1 where typical one dimensional wavenumber spectra of a TBL pressure field (at Mach 0.1) and a finite flat panel vibration response function are compared for a frequency of 500 Hz.

[1] dejong@calvin.edu

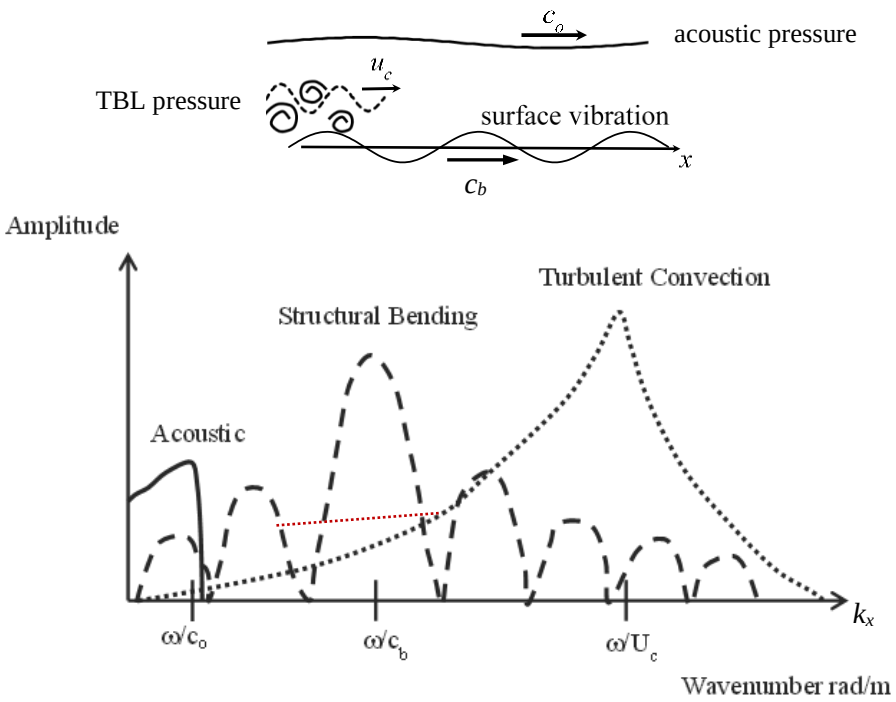

Figure 1. Spatial matching of wave fields as represented by their wavenumber spectra.
····· *Equation 1;* ····· *Typical TBL measurements*

The panel vibration is determined by the product of these two spectra which is dominated by two wavenumber regions: near the TBL convection peak and near the panel response peak. The latter is considered to be in the low wavenumber region of the TBL spectrum. Also shown is a typical spectrum of the acoustic pressure present which is usually much lower in amplitude than the TBL pressure but can also contribute to the panel vibration.

Measurements of the low wavenumber TBL pressure [2, 3, 4] generally have exceeded the levels predicted by Equation 1. Many attempts have been made to account for this difference [4, 5, 6]. The first part of this paper presents the results of new measurements from wind tunnel and closed water channel tests and proposes a theoretical basis for a modification to the basic Chase model.

The single point frequency spectrum of the TBL pressure, $\Phi_p(\omega)$, predicted by the basic Chase model is obtained by integrating Equation 1 over wavenumbers, resulting in

$$\Phi_p(\omega) = C' (\rho_o u_c^2)^2 [1 + (u_c / \delta \omega)^2]^{-3/2} / \omega \qquad (2)$$

Figure 2 compares this with typical measured results in a wind tunnel. It can be seen that the data falls off faster at high frequencies than Equation 2 predicts. Many attempts have been made to account for this difference [3, 6, 7, 8]. The second part of this paper presents the results of new measurements from wind tunnel and closed water channel tests and proposes a theoretical basis for a modification to the basic Chase model.

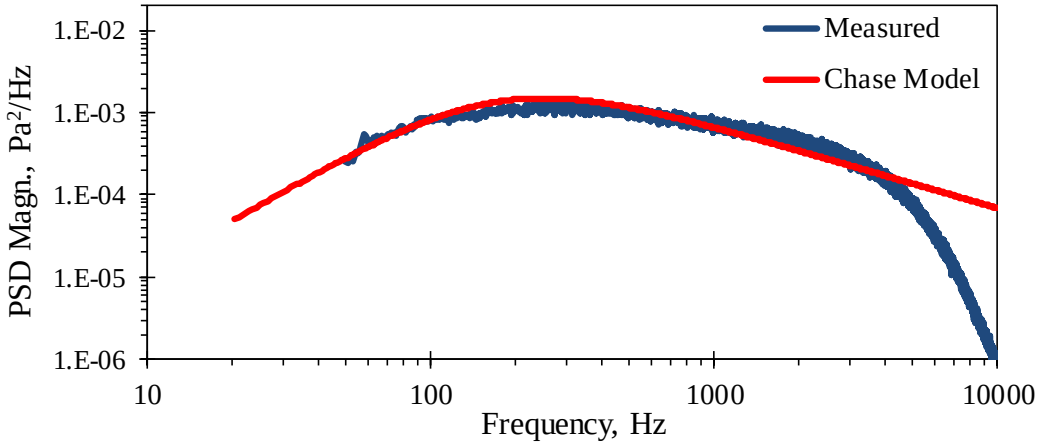

Figure 2. TBL pressure power spectral density (PSD) at 2.0 m with 20 m/s air flow

2. LOW WAVENUMBER TBL PRESSURE MEASUREMENTS AND ANALYSIS

The test results reported here use the method of Martin [2] to determine the low wavenumber component of the TBL pressure spectrum. The vibration response of a flat plate exposed to a TBL flow is used to back-calculated the TBL pressure levels at wavenumbers matching those of the bending vibration modes of the plate. Wind tunnel tests previously reported [4, 9, 10] have been extended to include more flat plate configurations to determine the low wavenumber component of the TBL pressure spectrum. The Calvin Engineering Department wind tunnel configuration is shown in Figure 3. Tests have been performed with variety of flat, rectangular plates constructed of steel, aluminum, glass, and polycarbonate, measuring 0.58 m by 0.18 m, with thicknesses varying from 0.61 mm to 4.0 mm, and positioned in the 3.0 m long test section at 0.9 m and 2.1 m downstream from the air flow inlet.

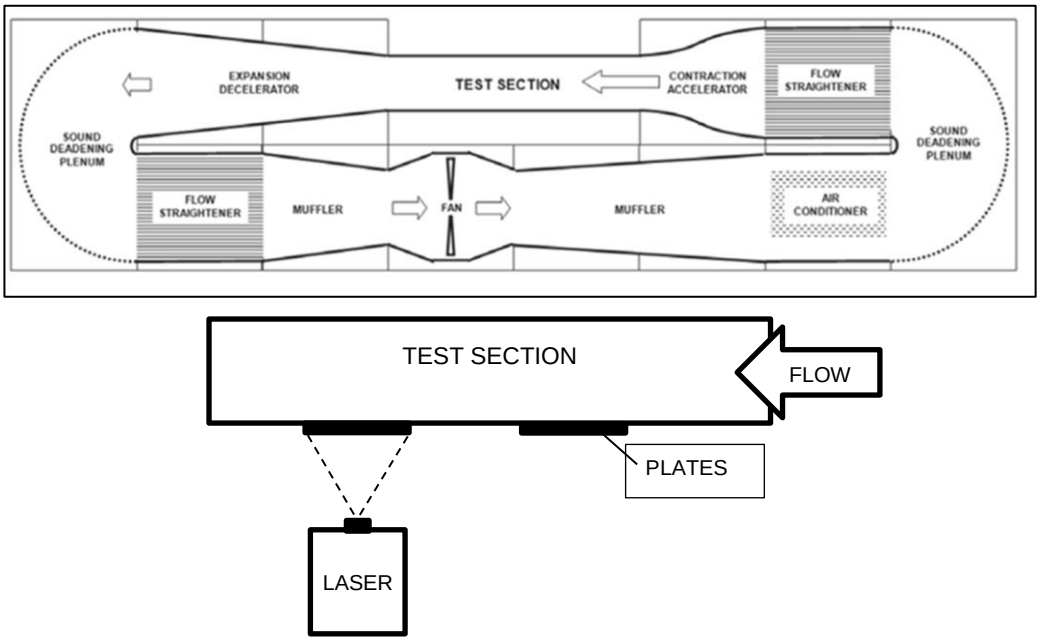

Figure 3. Calvin Engineering Department wind tunnel tests

The plates are supported around the perimeter with 25 x 50 mm steel beams, as shown in Figure 4, to approximate clamped edges. This minimizes the amplitude of the side bands in the wavenumber transform of the plate vibration mode shape [2] and makes them less susceptible to excitations at high wavenumbers. An example of a plate mode shape and corresponding two dimensional wavenumber spectrum, $\Psi(k,\omega)$, is shown in Figure 5. The mode shape is measured with a scanning laser vibrometer and acoustic excitation.

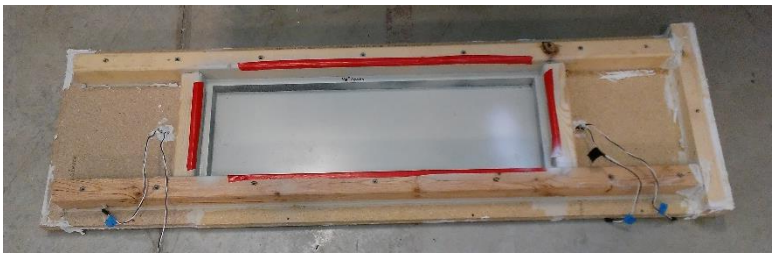

Figure 4. Typical test plate mounting with perimeter support beams

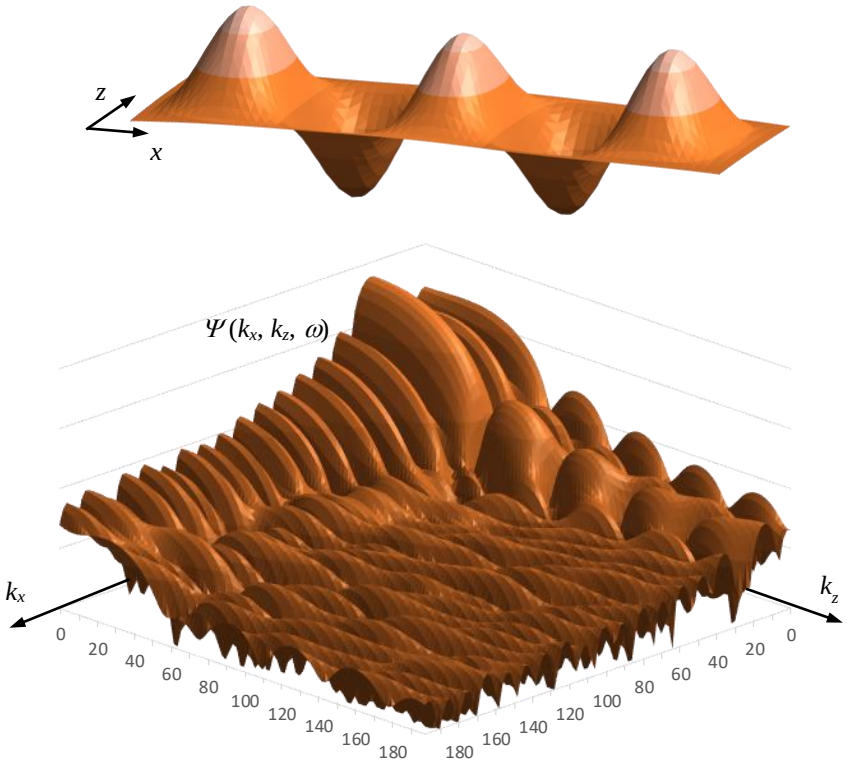

Figure 5. Measured mode shape and wavenumber spectrum of (5,1) mode of 3.5 mm glass panel at 1142 Hz

The frequency spectrum of the surface acceleration, $S_a(\omega)$, is then given by

$$\rho_s\, h_s\, \eta_s\, S_a(\omega) = \int \Phi_p(k,\omega)\, \Psi(k,\omega)\, dk \qquad (3)$$

where ρ_s, h_s, η_s are the plate density, thickness and damping, respectively.

With a plate installed in the wind tunnel flush to the test section wall (Figure 3) the acceleration spectrum is measured with a scanning laser vibrometer and the TBL pressure spectrum is back calculated using Equation 3 for each vibration mode. Figure 6 shows an example of a measured acceleration spectrum. There is enough frequency separation between most of the modes from 200 to 2000 Hz to determine their individual response levels. The damping loss values typically vary from 0.01 at lower frequencies to 0.002 at higher frequencies.

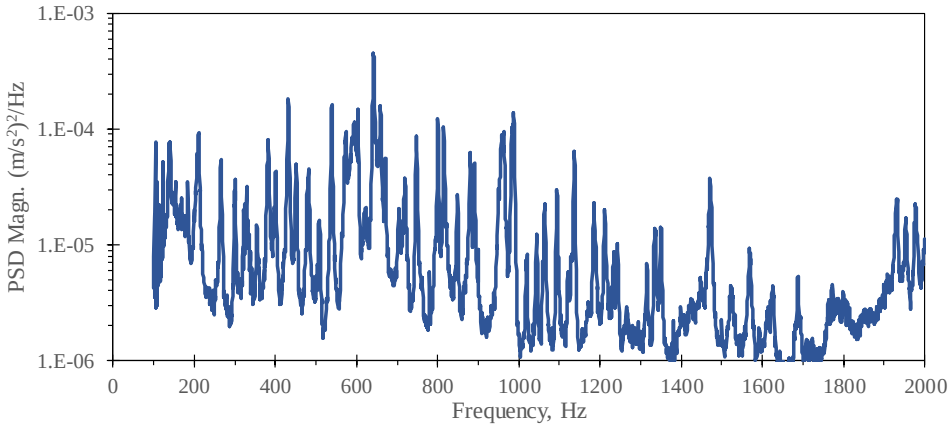

Figure 6. Measured power spectral density (PSD) of 0.61 mm steel plate acceleration level with 20 m/s air flow (0.625 Hz FFT bandwidth)

Even though the acoustic pressure is small compared to the turbulent pressure it can still contaminate the plate vibration measurement. This is because the acoustic pressure is concentrated at wavenumbers around k_o while the turbulent pressure is spread over a wavenumber range of about k_c. Previous tests in the wind tunnel [4] have shown the TBL/acoustic pressure ratio to be about 25 dB, and at 25 m/s the ratio of $(k_c/k_o)^2$ is 26 dB. To remove the acoustic contamination a method similar to Bonness [3] is used. A pressure transducer outside the TBL is used to measure the amount of plate vibration correlated with the acoustic pressure and this is removed from the measured vibration. Figure 7 shows an example of this. This usually only alters the data for the first few vibration modes at low frequencies.

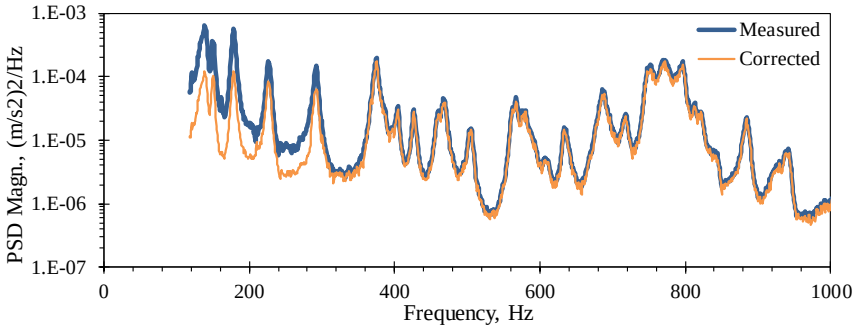

Figure 7. Measured and corrected PSD of 0.81 mm aluminum plate acceleration level with 25 m/s air flow.

New tests have also been performed using a closed water channel shown in Figure 8. The 3.0 m long test section consists of a lower half pipe (nominally 0.25 m diameter, schedule 80 PVC) with test plates rigidly attached to the top and supported by 38 mm by 50 mm beams around the perimeter. A variety of flat, rectangular plates constructed of steel, aluminum and brass, measuring 0.69 m by 0.15 m, with thicknesses of 0.81 mm to 3.2 mm, and positioned in the test section at 0.9 m and 2.1 m downstream from the water flow inlet have been tested. The supply tank provides gravity fed water from a height of about h = 2.5 m giving a theoretical maximum velocity of $(2\,g\,h)^{1/2}$ = 7.0 m/s. However, due to losses in the settling tank, the tests achieved a maximum velocity of 5.3 m/s. Lower speeds are achieved by partially closing the exit valves. The cross-sectional area of the lower half pipe increases by 20% along the length in order to account for the growth of the boundary layer at the wall and to achieve zero pressure gradient.

The water in the return pump section is isolated from the test water by using free, open flow in both the supply and discharge tanks. The pumps are enclosed in a noise and vibration isolation box. The 0.6 m x 0.6 m x 2.0 m settling tank is lined with crushed cell foam and steel mesh in order to dampen the acoustic waves in the test section. Also included is a flow straightening section and a 16:1 contraction section. Wire screen is used in all tanks to reduce the turbulence and eliminate entrained air bubbles. The vibration of the pipe sections is suppressed by surrounding them with sand.

The acceleration spectrum is measured with a scanning laser vibrometer and the TBL pressure spectrum is back calculated using Equation 3 for each vibration mode. Figure 9 shows an example of a measured acceleration spectrum. There is enough frequency separation between most of the modes from 50 to 1500 Hz to determine their individual response levels. The damping loss values typically vary from 0.02 at lower frequencies to 0.005 at higher frequencies. The surface mass includes fluid loading in this case.

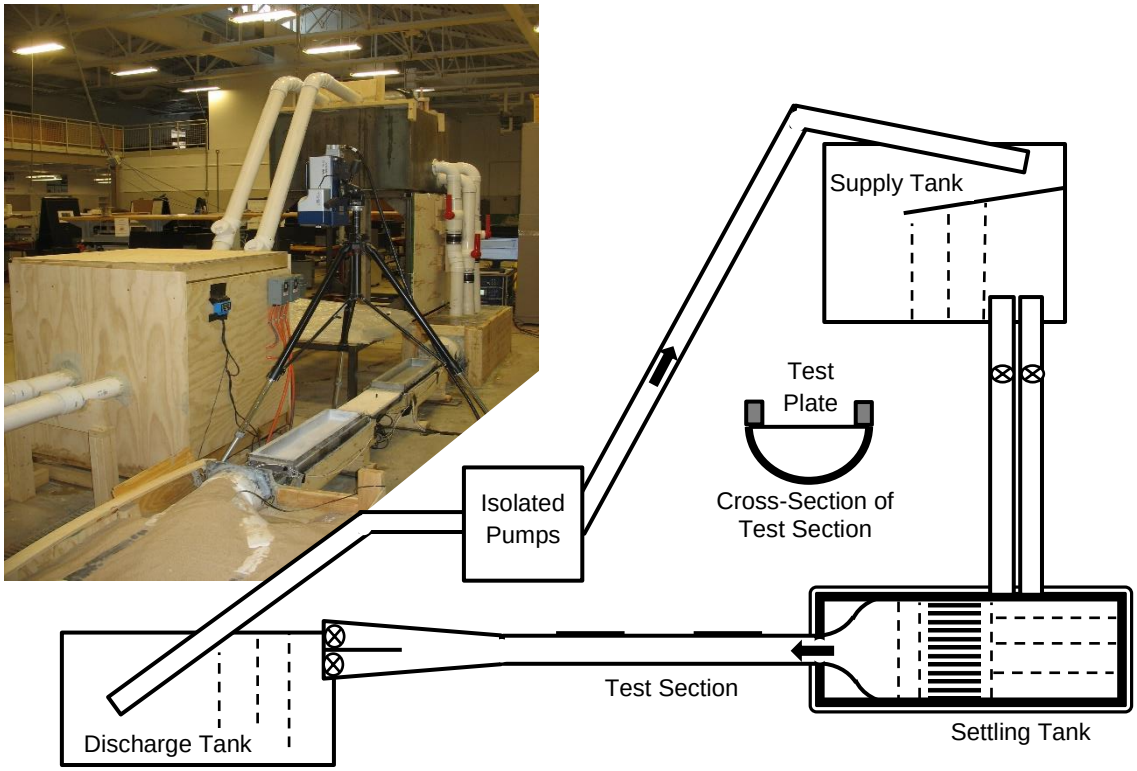

Figure 8. Water channel system using a closed top half-pipe

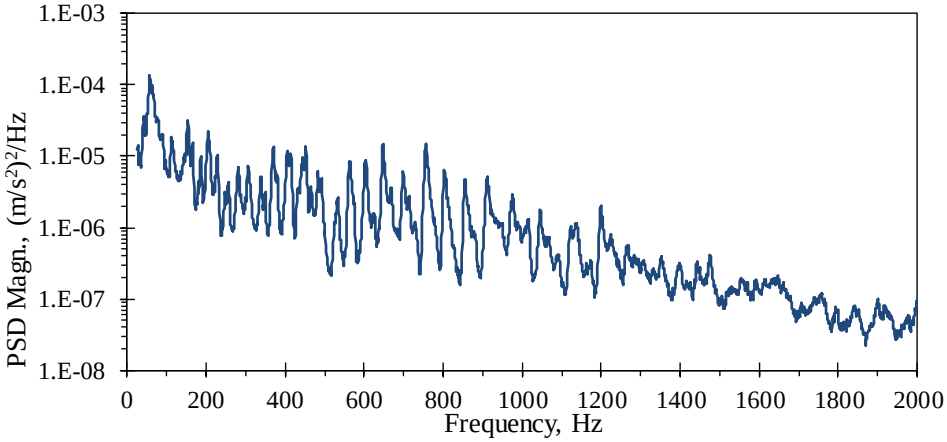

Figure 9. Measured power spectral density (PSD) of 0.81 mm brass plate acceleration level with 3.1 m/s water flow (0.625 Hz FFT bandwidth)

In this paper only the data obtained for purely axial wavenumbers are presented so $k = k_x$ and only the $(m,1)$ plate modes are considered. The TBL pressure spectrum is usually presented in non-dimensional form, but there are different forms of this in the literature. One form uses the "outer variables," the convection velocity, u_c, and the TBL displacement thickness, $\delta^* = \delta/8$. Focusing on the low wavenumber region ($k_x << \omega/u_c$), Equation 1 becomes (also with $\omega/u_c >> \delta^{-1}$)

$$\Phi_p(k_x,\omega)\, u_c / [\delta^3 (\rho_o u_c^2)^2] \sim C (2\pi)^{-5} (k/k_c)^2 / (\omega\delta/u_c)^3 \qquad (4)$$

where $k_c = \omega/u_c$.

Figure 10 presents the complete set of data for this condition with the normalized pressure spectrum plotted against the normalized axial wavenumber for different values of $\omega\delta/u_c$.

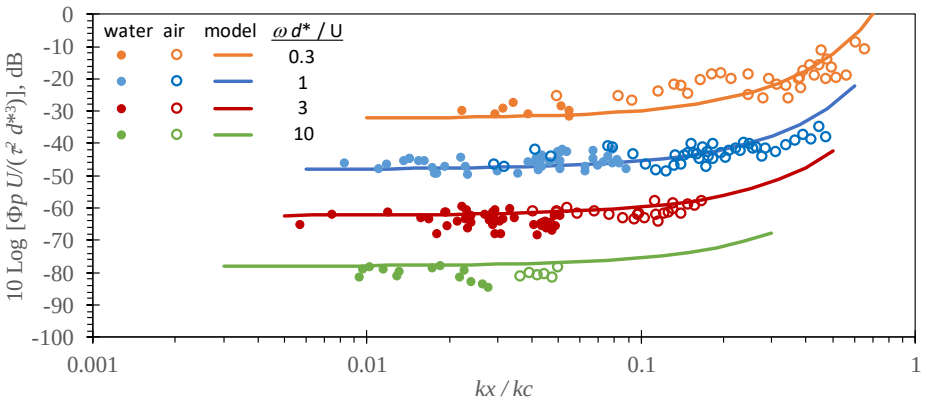

Figure 10. Measured TBL spectra and model curve fit

The data show no strong dependence on k for $k << k_c$ where as Equation 4 predicts a k^2 dependence. This is consistent with other measurements [2, 3]. A theorem by Kraichnan [11] is often sited as the reason for the k^2 dependence in theoretical results. This is derived for a uniform boundary layer over an infinite flat surface with a constant

thickness and mean flow parallel to the surface. Then there can be no spatially uniform ($k_x = 0$), non-zero pressure against the surface. However, in reality the boundary layer is growing and new kinetic energy is entering the boundary layer at a nearly uniform rate spatially. This is illustrated in Figure 11.

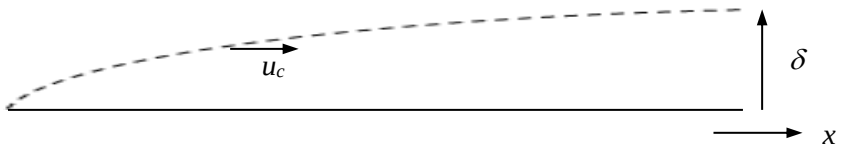

Figure 11. Illustration of growth of TBL and addition of kinetic energy, ½ $\rho_o u_c^2$

An approximation for the spatially uniform pressure is

$$p \sim \rho_o u_c^2 \, d\delta/dx \tag{5}$$

and the growth of the boundary layer profile is approximated by

$$\delta = 0.16 \, x \, \mathrm{Re}^{-1/7} = 0.16 \, x^{6/7} \, (\nu/U)^{1/7} \tag{6}$$

where the Reynolds number is $\mathrm{Re} = U x / \nu$, U is the free stream velocity and ν the fluid kinematic viscosity.

Then

$$p \sim \rho_o u_c^2 \, (\mathrm{Re})^{-1/7} \tag{7}$$

which has a very weak dependence on x. Approximating the Fourier transforms of p^2 gives

$$\Phi_p(k,\omega) \sim (\rho_o u_c^2)^2 / \omega \, k_c^2 \tag{8}$$

which can be included in Equation 1 by adding a term to the numerator proportional to k_c^2. By curve fitting this to the data in Figure 10 a scaling of $1/\pi$ is determined. The revised model is then

$$\Phi_p(k,\omega) = C \, \rho_o^2 \, u_c^3 \, (k^2 + k_c^2/\pi)[k^2 + (2\pi)^2 \, (\omega/u_c - k_x)^2 + \delta^{-2}]^{-5/2} \tag{9}$$

which is also plotted in Figure 10.

3. HIGH FREQUENCY TBL PRESSURE MEASUREMENTS AND ANALYSIS

Figure 2 illustrates the inadequacy of the basic Chase model for the TBL pressure spectrum at high frequencies. Most attempts to fix this [3, 6, 7, 8] have added an empirically derived term to roll off the model at high frequencies. One of the difficulties in obtaining reliable high frequency data is the reduced sensitivity of a microphone surface when the diameter, d, is a significant fraction of the turbulent eddy size, $k_c \, d > 1$. Up to $k_c \, d = 2\pi$ the reduced sensitivity can be corrected [12]. In the measurements reported here the microphones are mounted behind a pin hole with $d = 0.8$ mm and all the data have been corrected for its response function..

The appropriate variables for the high frequency scaling can be found by looking at the measured pressure spectra using different scaling parameters. Figure 12 shows an example of the measured TBL pressure spectra at one location and four flow velocities scaled by the outer variables, u_c and δ^*.

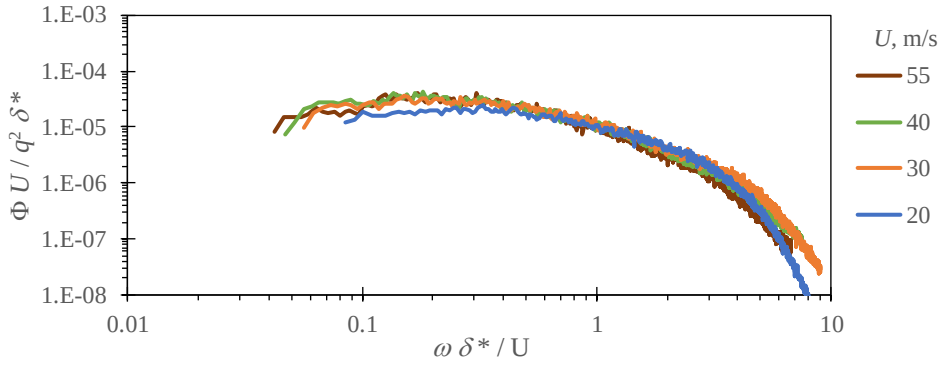

Figure 12. Measured TBL pressure spectra at 1.8 m position in wind tunnel with four air flow speeds, normalized by the outer variables ($q = ½ \rho U^2$)

The normalization looks good except for the fact that δ^* is not varying. Figure 13 shows an example of the measured TBL pressure spectra at four locations and one flow velocity scaled by the outer variables. Here the frequency scaling does not collapse the data at high frequencies.

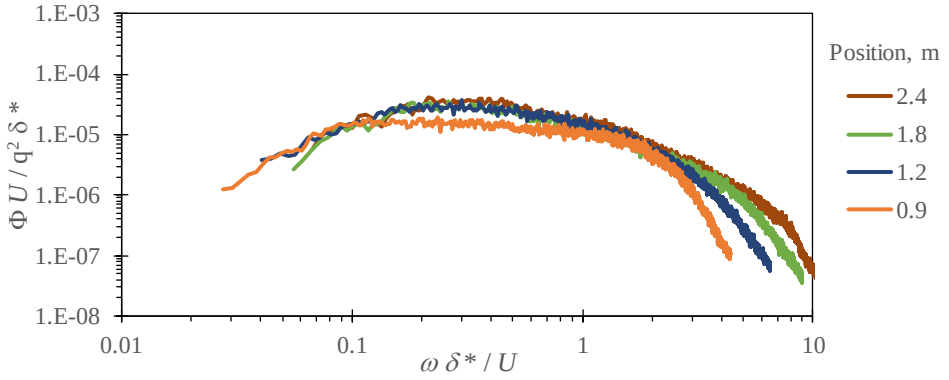

Figure 13. Measured TBL pressure spectra at four positions in wind tunnel with 30 m/s air flow speed, normalized by the outer variables ($q = ½ \rho U^2$)

Another choice of scaling parameters that has been found to work at high frequency uses the inner variables; fluid kinematic viscosity, ν, and surface shear stress, $\tau_w = \rho_o u_t^2$, or just u_t the friction velocity [3, 6, 7, 12]. Figure 14 shows a set of measured TBL pressure in both air and water normalized by these variables. The high frequency data collapse but the low frequency data do not.

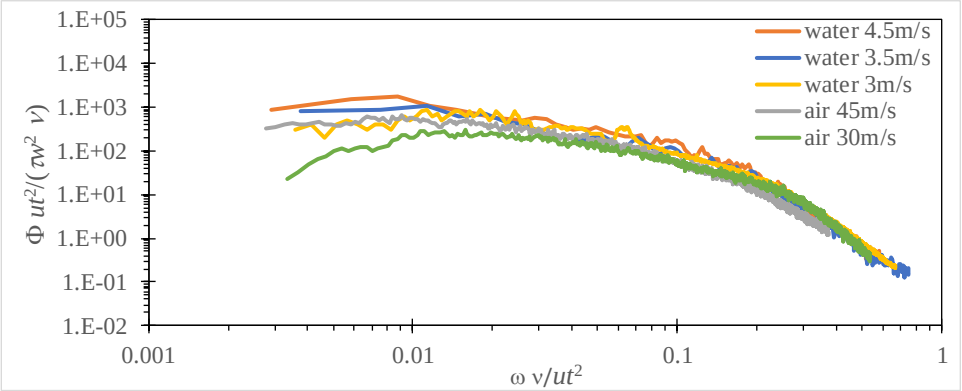

Figure 14. Measured TBL pressure spectra in both wind an water tunnel normalized by the inner variables, ν, and $\tau_w = \rho_o u_t^2$

This indicates that ν/u_t is the length scale for the high frequency normalization. In a TBL the inner most shear layer at the surface is usually determined to have a thickness of about $6\nu/u_t$. In the development by Chase [1] of Equation 1, the last step uses an integral of the form

$$\Phi_p(k,\omega) = C' \rho_o^2 u_c^3 k^2 \int [k_y^2 + k^2 + (2\pi)^2 (\omega/u_c - k_x)^2 + \delta^{-2}]^{-3} d k_y \qquad (10)$$

Neglecting the effects of the shear layer this integral is evaluated to infinity for k_y, the wavenumber perpendicular to the surface. However, as Chase suggests, one of the effects of the shear layer is to supress the small scale turbulent eddies and reduce the high frequency pressure spectrum. To approximate this effect the integral in Equation 10 can be evaluated to limiting values of $+/- u_t/6\nu$. In doing so a factor of $[1 + k^2 (6\nu/u_t)^2]^{-2}$ is appended to Equation 1.

Integrating this over wavenumber to obtain the frequency spectrum gives

$$\Phi_p(\omega) = C' (\rho_o u_c^2)^2 / \{\omega ([1 + (u_c/\delta\omega)^2]^{3/2} + [6\omega\nu/u_t^2]^4)\} \qquad (11)$$

This revised Chase model is plotted along with a TBL pressure measurement in water in Figure 15 showing excellent agreement.

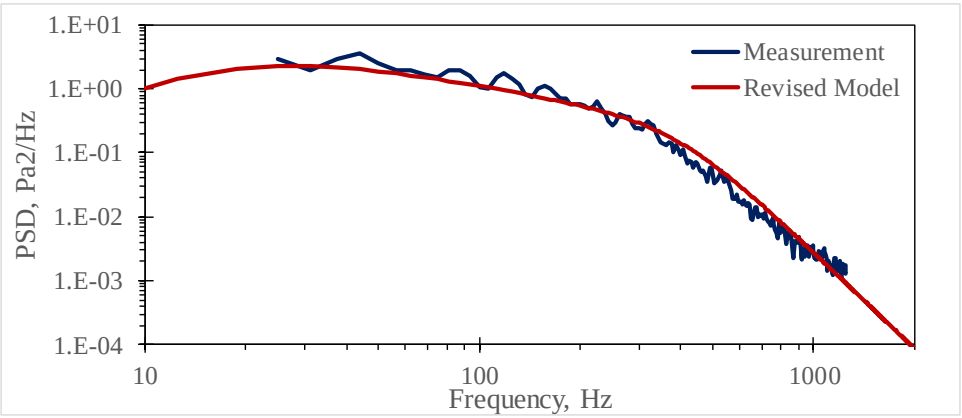

Figure 15. Measured TBL pressure spectra in water tunnel compared to the revised Chase model (Equation 11, $C' = 10^{-5}$)

4. CONCLUSIONS

Measurements of the TBL pressure and plate vibration in both wind tunnel and closed water channel have been used to extend the basic Chase model to more accurately represent the low wavenumber and high frequency regions. Theoretical justifications for these modifications are used to infer the best scaling parameters to be used.

5. ACKNOWLEDGEMENTS

This work was made possible by the research support from Spirit AeroSystems, Northrop Grumman Marine Systems, and Toyota Motor Engineering & Manufacturing North America.

6. REFERENCES

1. D. Chase, "Modeling the wave-vector frequency spectrum of turbulent boundary layer wall pressure," *J. Sound Vib.*, **70**, 29–68 (1980)
2. N. Martin and P. Leehey, "Low wavenumber wall pressure measurements using a rectangular membrane as a spatial filter," *J. Sound Vib.*, **52**, 95–120 (1977)
3. W. Bonness, D. Capone, and S. Hambric, "Low-wavenumber turbulent boundary layer wall-pressure measurements from vibration data on a cylinder in pipe flow," *J. Sound Vib.*, **329**, 4166–4180 (2010)
4. R. DeJong and S. Sorenson, "Low wavenumber pressure content of turbulent boundary layer flows," *Proceedings Inter-Noise 2018*, Chicago (2018)
5. D. Chase, "The character of the turbulent wall pressure spectrum at subconvective wavenumbers and a suggested comprehensive model," *J. Sound Vib.*, **112**(1), 125-147 (1987)
6. T. Miller, *et al*. "Review of turbulent boundary layer models for acoustic analysis," *Journal of Aircraft*, **49**(6) (2012)
7. M. Goody, "Empirical spectral model of surface pressure fluctuations," *AIAA Journal*, **42**(9) 1788-1794 (2004)
8. R. DeJong, "Wind noise modeling in separated and reattaching boundary layers," *Proceedings Inter-Noise 2016*, Hamburg (2016)
9. R. DeJong and I. Kuiper, "Pressure gradient effects on turbulent pressure spectrum," *Proceedings Inter-Noise 2012*, New York City (2012)
10. M. Moeller, *et al.*, "Effect of developing pressure gradients on TBL wall pressure spectrums," *Proceedings FLINOVIA*, Rome (2013)
11. R. Kraichnan, "Pressure fluctuations in a turbulent flow over a flat plate," *J. Acoust. Soc. Am.*, **28** 378-390 (1956)
12. W. Blake, *Mechanics of Flow-Induced Sound and Vibration*, 2nd ed., vol.2, chap. 2, Academic Press, Cambridge, MA (2017)